ACS Photonics

Letter

pubs.acs.org/journal/apchd5

High-Performance Flexible Perovskite Solar Cells by Using a Combination of Ultrasonic Spray-Coating and Low Thermal Budget Photonic Curing

Sanjib Das,[†] Bin Yang,[‡] Gong Gu,[†] Pooran C. Joshi,[§] Ilia N. Ivanov,[‡] Christopher M. Rouleau,[‡] Tolga Aytug,[⊥] David B. Geohegan,[‡] and Kai Xiao*[,‡]

[†]Department of Electrical Engineering and Computer Science, University of Tennessee, Knoxville, Tennessee 37996, United States
[‡]Center for Nanophase Materials Sciences, [§]Materials Science and Technology Division, and [⊥]Chemical Sciences Division, Oak Ridge National Laboratory, Oak Ridge, Tennessee 37831, United States

Supporting Information

ABSTRACT: Realizing the commercialization of high-performance and robust perovskite solar cells urgently requires the development of economically scalable processing techniques. Here we report a high-throughput ultrasonic spray-coating (USC) process capable of fabricating perovskite film-based solar cells on glass substrates with a power conversion efficiency (PCE) as high as 13%. Perovskite films with high uniformity, crystallinity, and surface coverage are obtained in a single step. Moreover, we report USC processing on TiO_2/ITO-coated polyethylene terephthalate (PET) substrates to realize flexible perovskite solar cells with a PCE as high as 8.1% that are robust under mechanical stress. In this case, a photonic curing technique was used to achieve a highly conductive TiO_2 layer on flexible PET substrates for the first time. The high device performance and reliability obtained by this combination of USC processing with optical curing appear very promising for roll-to-roll manufacturing of high-efficiency, flexible perovskite solar cells.

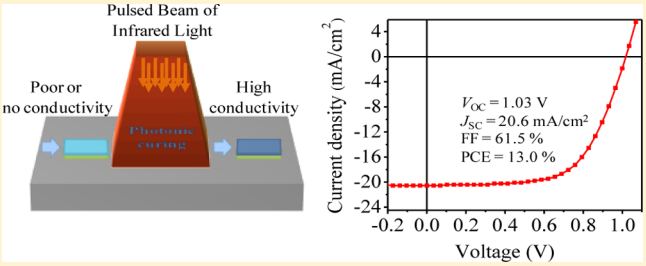

KEYWORDS: *perovskite solar cell, ultrasonic spray-coating, photonic curing technique*

Organometallic trihalide perovskite solar cells, with power conversion efficiencies (PCEs) rapidly reaching ca. 20%,[1−3] are one of the most promising, next-generation photovoltaic technologies due to their excellent material properties, including long carrier diffusion lengths[4] and large absorption coefficients.[5] To achieve high-quality perovskite films, a variety of deposition techniques, such as thermal evaporation,[6−8] single-step spin-coating,[9,10] layer-by-layer or two-step coating,[11,12] and vapor-assisted[13] processes, have been developed. However, one major disadvantage of most laboratory-scale techniques is that they are incompatible with low-cost, roll-to-roll processing envisioned for large-scale manufacturing. Existing scalable processing techniques include inkjet printing, slot-die coating, blade-coating, screen printing, and ultrasonic spray-coating.[14−21]

Among these cost-effective roll-to-roll compatible processes, ultrasonic spray-coating (USC) is one of the most promising that has been successfully exploited for the fabrication of various organic electronic devices including light-emitting diodes,[22] photovoltaics,[23,24] photodetectors,[25] and field-effect transistors.[26] The overall advantage of USC is its ability to simultaneously provide high throughput, better control over directional deposition, efficient use of materials, uniform film coverage, and compatibility with a variety of substrates, with the potential for the deposition of continuous layers without dissolution of underlying layers.[23,26−28] Recently, the USC process was demonstrated to deposit perovskite thin films on glass substrates, and the resulting devices showed an average PCE of 7.8%.[29]

However, considering the diverse application potential for thin-film perovskites, it is highly important to demonstrate the fabrication of high-performance devices on lightweight and flexible substrates using scalable techniques. So far, one major challenge for the fabrication of solar cells on plastic substrates is their incompatibility with high temperature. Typically, the fabrication of high-performance perovskite solar cells, particularly those based on high-quality compact TiO_2 electron-transporting layers, involves a high-temperature (∼500 °C) sintering process to increase the crystallinity of TiO_2.[2,4,6]

In this work, we report a USC process for the synthesis of highly crystalline and uniform $CH_3NH_3PbI_{3-x}Cl_x$ films, suitable for the fabrication of solar cells on glass substrates with a PCE measured as high as 13% and an average in all runs of 10.6%. To realize flexible solar cells, a photonic curing technique that is compatible with roll-to-roll processing was used to achieve conductive TiO_2 layers on ITO-coated polyethylene terephthalate (PET) substrates at low processing temperatures. Solar

Received: March 12, 2015
Published: May 25, 2015

DOI: 10.1021/acsphotonics.5b00119
ACS Photonics 2015, 2, 680−686

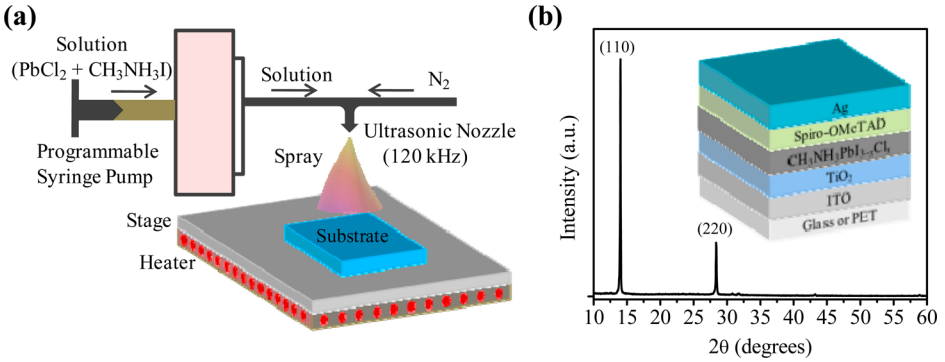

Figure 1. (a) Schematic diagram of ultrasonic spray-coating process. (b) XRD pattern of a spray-coated $CH_3NH_3PbI_{3-x}Cl_x$ film. The inset of (b) schematically shows the device architecture.

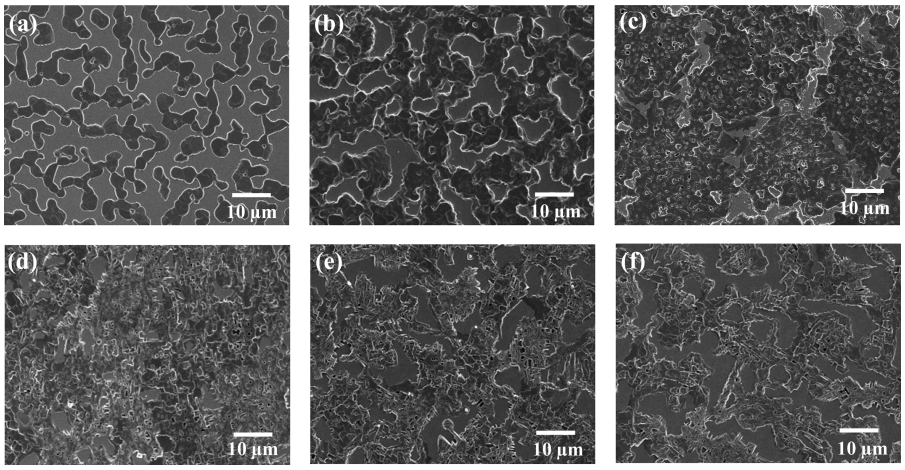

Figure 2. SEM images of spray-coated perovskite films on TiO_2/ITO/glass substrates at different substrate temperatures: (a) 26 °C, (b) 45 °C, (c) 60 °C, (d) 75 °C, (e) 90 °C, and (f) 105 °C.

cells fabricated on PET substrates exhibited PCEs as high as 8.1%, which stayed at about 60−90% of their peak efficiencies after more than 1000 bending cycles.

Figure 1a schematically shows the USC process, where the solution is fed through a programmable syringe pump and sprayed using a 120 kHz ultrasonic nozzle. The nozzle atomizes the solution into micrometer-size droplets with the help of an atomizing nitrogen-gas pressure that prevents clogging of the solution in the nozzle-head. In our work, a solution mixture of methylammonium iodide (CH_3NH_3I) and lead chloride ($PbCl_2$) precursors was ultrasonically spray-coated on various substrates, and then the obtained films were thermally annealed at 100 °C for 1 h in air to drive the chemical reaction and crystallization. The annealed, spray-coated film shows strong and sharp Bragg peaks (Figure 1b) at 14.1° and 28.4°, corresponding to (110) and (220) planes, respectively, indicating the formation of a highly crystalline tetragonal perovskite film.[5,29]

In order to achieve high-quality perovskite films for high-performance devices, we optimized the USC process by comparing different solvents, tuning the substrate temperature, and optimizing the perovskite film thickness. To examine the effect of solvent, we used two solvents with different boiling points: *N*,*N*-dimethylformamide (DMF, boiling point = ∼153 °C) and dimethyl sulfoxide (DMSO, boiling point = ∼189 °C). The high boiling points of these solvents result in prolonged drying times (∼15 min for DMF and ∼25 min for DMSO) for the coated films. To minimize the drying time, we used elevated substrate temperatures in conjunction with a lower boiling point solvent, DMF. A scanning electron microscope (SEM) image (Figure 2a) shows that the film, spray-coated on a TiO_2/ITO/glass substrate at room temperature (26 °C), exhibits low surface coverage due to the dewetting caused by the prolonged drying time. As shown in Figure 2b−f, elevated substrate temperatures result in improved film coverage by reducing the surface tension of the wet film; however temperatures of >90 °C again result in lower film coverage due to immediate drying of the solution upon reaching the substrate. Figure 3 shows the variation of device performance corresponding to these changing substrate temperatures. Although the open-circuit voltage (V_{OC}) and fill factor (FF) exhibit negligible differences with increasing substrate temperature, the short-circuit current density (J_{SC}) reaches the highest value, 13.8 mA/cm^2, at 75 °C, which corresponds to the perovskite films with the highest surface coverage on the TiO_2 layer.

By comparison, films coated using a relatively high boiling point solvent, DMSO, exhibit lower surface coverage (see Supporting Information, Figure S1) compared to the films coated using DMF (Figure 2). These differences are reflected in the device performance, as shown in Table S1. The DMSO-processed perovskite films result in an average PCE of only 4.2%, whereas DMF-processed films show an average PCE of 8.2%, a 95% enhancement. This large efficiency enhancement is mainly ascribed to significant enhancements in J_{SC} and V_{OC} by 59% and 23%, respectively, which result from the fast evaporation of the low-boiling-point solvent DMF, leading to

DOI: 10.1021/acsphotonics.5b00119
ACS Photonics 2015, 2, 680−686

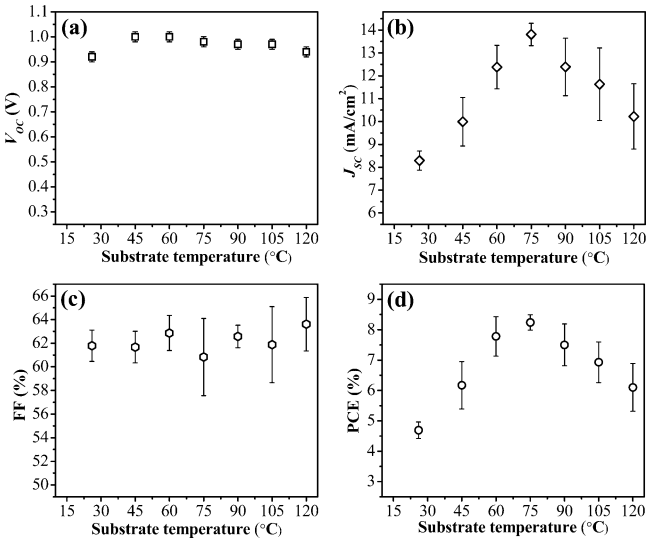

Figure 3. Device performance parameters, i.e., (a) V_{OC}, (b) J_{SC}, (c) FF, and (d) PCE, at different substrate temperatures. Device performance from 120 °C is included to illustrate the trend.

fast crystallization and better surface coverage of $CH_3NH_3PbI_{3-x}Cl_x$ films.[9,29] For the subsequent optimization of the USC process described below, therefore, the substrate temperature was fixed at 75 °C, and DMF was used as the solvent.

To further enhance the film properties and device performance, we optimized the perovskite film thickness by varying the solution concentration and infusion rate. Two important observations are made, as shown in Table 1. First, the film roughness increases with increasing the thickness of the perovskite films. Second, the variation of film thickness primarily impacts the J_{SC}. We found that the J_{SC} steadily increases with increasing film thickness, which we attribute to enhanced photonic absorption. The highest J_{SC} of 19.3 mA/cm^2 and thus the highest PCE of 11.4 ± 0.4% are reached when the film thickness is increased to 295 ± 33 nm. However, the J_{SC} decreases with further increasing the thickness, probably due to higher charge recombination.[30−32]

To correlate the USC process optimization with the device performance and also provide a measure of reproducibility, a series of devices were fabricated on glass substrates. The current density versus voltage (J−V) curve of a typical solar cell is shown in Figure 4a, with a J_{SC} of 18 mA/cm^2, V_{OC} of 1.05 V, FF of 60.7%, and PCE of 11.5% at forward bias (FB) to reverse bias (RB) scanning direction and a J_{SC} of 18 mA/cm^2, V_{OC} of 1.00 V, FF of 61.2%, and PCE of 11.1% at a RB−FB direction, under AM 1.5G (100 mW/cm^2) illumination, measured in a nitrogen-filled glovebox. This small hysteresis may be attributed to use of planar device architecture.[35,34] In order to better evaluate the performance, we also determined the stabilized current density and power output (Figure 4b) of this device by measuring current density at around maximum power point (∼0.75 V), which gives a similar PCE of 11%. The external quantum efficiency (EQE) spectrum of the same device measured in air without encapsulation is shown in Figure 4c, where integrating the EQE curve over the spectral range (AM 1.5G) yielded a J_{SC} of 17.14 mA/cm^2, ∼4.7% lower than the J_{SC} extracted from J−V characteristics, which could be due to the mismatch in two different solar spectra[3] or instability of Spiro-OMeTAD in air.[33] To demonstrate the statistical significance of the high device performance obtained by process optimization, Figure 4d shows a PCE histogram of 60 devices fabricated on glass substrates using the optimized process. The most efficient cell exhibits a J_{SC} of 20.6 mA/cm^2, V_{OC} of 1.03 V, FF of 61.6%, and PCE of 13% (Figure S2). These devices demonstrate an average PCE of 10.6 ± 1.0%, which is comparable to that of the devices fabricated by spin-coating (Figure S3). The statistically significant results clearly reveal the potential of USC in the large-scale manufacturing of perovskite solar cells.

The excellent device performance discussed above encouraged us to fabricate devices on flexible and lightweight PET substrates. Instead of the high-temperature annealing (∼500 °C) of the TiO_2 films used for glass substrates,[2,4,6] we used a photonic curing technique to achieve conductive TiO_2 films on ITO/PET substrates, where the TiO_2 films are exposed to 5 to 10 high-density infrared (HDI) light pulses from a high-intensity plasma arc lamp for short dwell times of 1−2 ms. This technique, also called pulse-thermal processing (PTP), is a HDI processing technology based radiant heat treatment technique that can deliver a peak sintering power up to 20 000 W/cm^2 during a millisecond and is used to rapidly anneal thin films of various materials without damaging underlying plastic substrates.[36,37] This tool enables reproducible, roll-to-roll, high-temperature processing of thin-film materials on low-temperature substrates. Figure 5a shows the simulated temperature-versus-time profile for the photonic curing technique used in this work to anneal TiO_2 films on ITO-coated PET substrates. Figure 5b shows the J−V curves for the best devices with as-spin-coated, thermally annealed, and photonic-cured TiO_2 films. As can be seen, the device with an as-coated TiO_2 film shows very poor photovoltaic performance: J_{SC} = 3.2 mA/cm^2, V_{OC} = 0.78 V, FF = 15.1%, and PCE = 0.4%. This poor performance, particularly very low J_{SC} and FF, is due to the high interfacial resistance in the device due to poor conductivity of TiO_2 films. The device using thermally annealed TiO_2 shows a J_{SC} = 3.5 mA/cm^2, V_{OC} = 1.04 V, FF = 48.7%, and PCE = 1.8%, a five-times improvement. On the other hand, the device with

Table 1. Summary of Device Parameters, i.e., J_{SC}, V_{OC}, FF, and PCE, of the Perovskite Solar Cells Fabricated with Different Perovskite Film Thicknesses

infusion rate [mL/min]	solution concentration [wt %]	film thickness [nm]	J_{SC} [mA/cm^2]	V_{OC} [V]	FF [%]	PCE$_{av}$[a] [%]
2.6	8	165 ± 18	15.6 ± 1.9	1.03 ± 0.05	62.0 ± 1.6	10.0 ± 2.0
2.6	10	236 ± 21	16.0 ± 2.6	0.98 ± 0.07	64.0 ± 1.2	10.1 ± 2.3
3.2	10	295 ± 33	19.3 ± 0.7	0.97 ± 0.03	60.8 ± 2.2	11.4 ± 0.3
2.6	12	408 ± 54	16.8 ± 0.9	0.97 ± 0.02	61.4 ± 1.8	10.0 ± 0.2
3.2	12	440 ± 83	17.1 ± 2.2	0.97 ± 0.10	59.4 ± 8.0	9.9 ± 2.4
4.4	12	501 ± 180	17.2 ± 1.7	0.95 ± 0.06	59.6 ± 5.0	9.7 ± 2.0

[a]Average PCEs are based on eight devices with each thickness.

DOI: 10.1021/acsphotonics.5b00119
ACS Photonics 2015, 2, 680−686

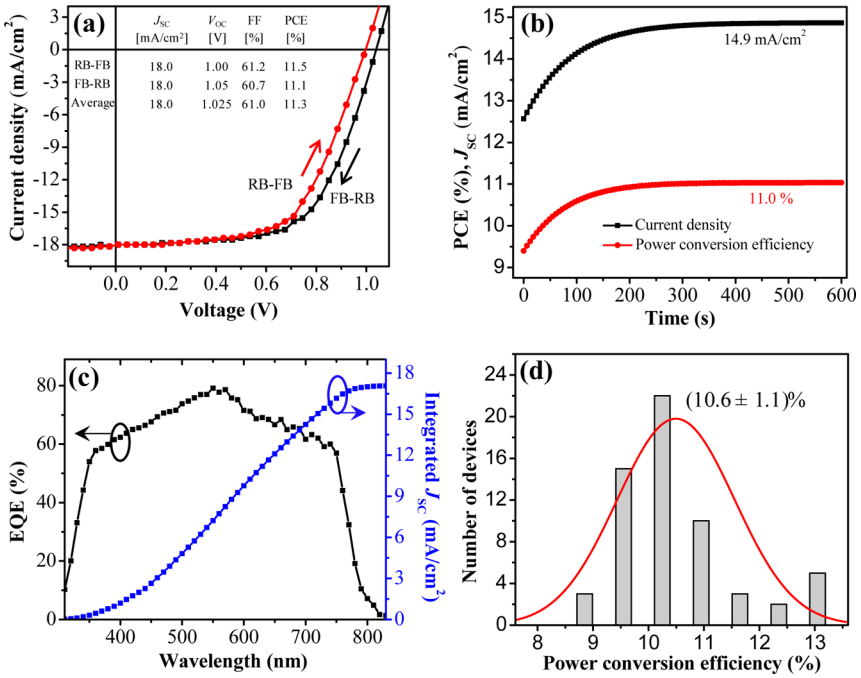

Figure 4. (a) $J-V$ curve of a typical perovskite solar cell on a glass substrate at different scanning directions. (b) Current density and PCE as a function of time for the same device held at 0.75 V forward bias. (c) EQE spectrum and integrated J_{SC} from the corresponding device under short-circuit conditions. (d) Histogram of PCEs measured for 60 devices, fabricated with an optimized USC process. Gaussian fit is provided as a guide to the eyes.

photonic-cured TiO_2 exhibits excellent performance, with a J_{SC} = 15.3 mA/cm^2, V_{OC} = 1.03 V, FF = 51.4%, and PCE of 8.1%, measured at an FB−RB scanning direction under AM 1.5G illumination in a nitrogen-filled glovebox. At an RB−FB scanning direction, however, the device shows a J_{SC} = 15.1 mA/cm^2, V_{OC} = 0.98 V, FF = 46.9%, and an overall PCE of only 6.9%, showing pronounced hysteresis, probably due to the use of planar device architecture.[35,34] The stabilized current density and power output from the same device at maximum power point (~0.61 V) are 12 mA/cm^2 and 7.3%, respectively (Figure 5c), which gives a reasonably accurate estimate of the device performance. The integrated J_{SC} from the EQE spectrum (Figure 5d) from the same device is 15.1 mA/cm^2, which is well consistent with the measured J_{SC} from $J-V$ characteristics.

To demonstrate the mechanical flexibility, a stringent bending test was performed on four flat flexible devices at 7 mm and 3 mm radii of curvature (Figure 5e). The devices retain 60−90% of their initial PCEs after 1000 bending cycles, demonstrating the compatibility of perovskite solar cells with low-cost and lightweight flexible substrates. The small degradation in device performance results from a decrease in J_{SC} and FF due to cracking of ITO at higher stress (Figure S8) and increased contact resistance. Overall, flexible devices exhibit an excellent average PCE of 5.9% (Figure 5f). Although the average J_{SC} and FF of devices on PET substrates (Table S3) are lower than those on glass substrates, due to lower conductivity of the photonic-cured TiO_2 as compared to the thermally annealed TiO_2 on glass, the reasonably high PCEs of flexible devices fabricated using a combination of USC process and the photonic curing technique represent a substantial step toward the mass production of perovskite solar cells in the near future.

In summary, a high-throughput ultrasonic spray-coating process was successfully applied to fabricate high-quality, uniform, and highly crystalline $CH_3NH_3PbI_{3-x}Cl_x$ films on glass substrates for solar cell applications. The best solar cell fabricated on glass exhibited an efficiency of 13%, comparable to that of a $CH_3NH_3PbI_{3-x}Cl_x$ device made by spin-coating. The spray-coating process flow has also been successfully translated from glass substrates to plastic PET substrates. Together with a low-temperature photonic-cured compact TiO_2 layer, the best flexible $CH_3NH_3PbI_{3-x}Cl_x$ solar cell, fabricated by spray-coating, exhibited a PCE as high as 8.1%. The excellent mechanical flexibility of these devices was demonstrated by the minimal degradation in performance after more than 1000 bending cycles. The scalability of the spray-coating process together with a low thermal budget photonic curing technique used in this work for the development of high-performance flexible perovskite solar cells represents a very unique and viable route for the roll-to-roll manufacturing of new-generation solar cells.

EXPERIMENTAL SECTION

Materials and Solution Preparation. TiO_2 for the electron transport layer was synthesized following a method published elsewhere.[10] $CH_3NH_3PbI_{3-x}Cl_x$ precursors, methylammonium iodide (MAI) and lead chloride ($PbCl_2$), were purchased from 1-Material and Sigma-Aldrich, respectively, and used as received. MAI was mixed with $PbCl_2$ (3:1 molar ratio) and dissolved in anhydrous DMF for a total concentration of 10 wt %. Hole transport material, 2,2′,7,7′-tetrakis(*N*,*N*-dimethoxyphenylamine) 9,9′-spirobifluorene (Spiro-OMeTAD, 1-Material), was dissolved in chlorobenzene for a concentration of 90 mg/mL and doped with 45 μL of lithium bis(trifluoromethanesulfonyl)imide (LiTFSI) solution (170 mg/mL in acetonitrile) and 10 μL of 4-*tert*-butylpyridine (tBP) solution. Both LiTFSI and tBP were purchased from Sigma-Aldrich and used as received.

DOI: 10.1021/acsphotonics.5b00119
ACS Photonics 2015, 2, 680−686

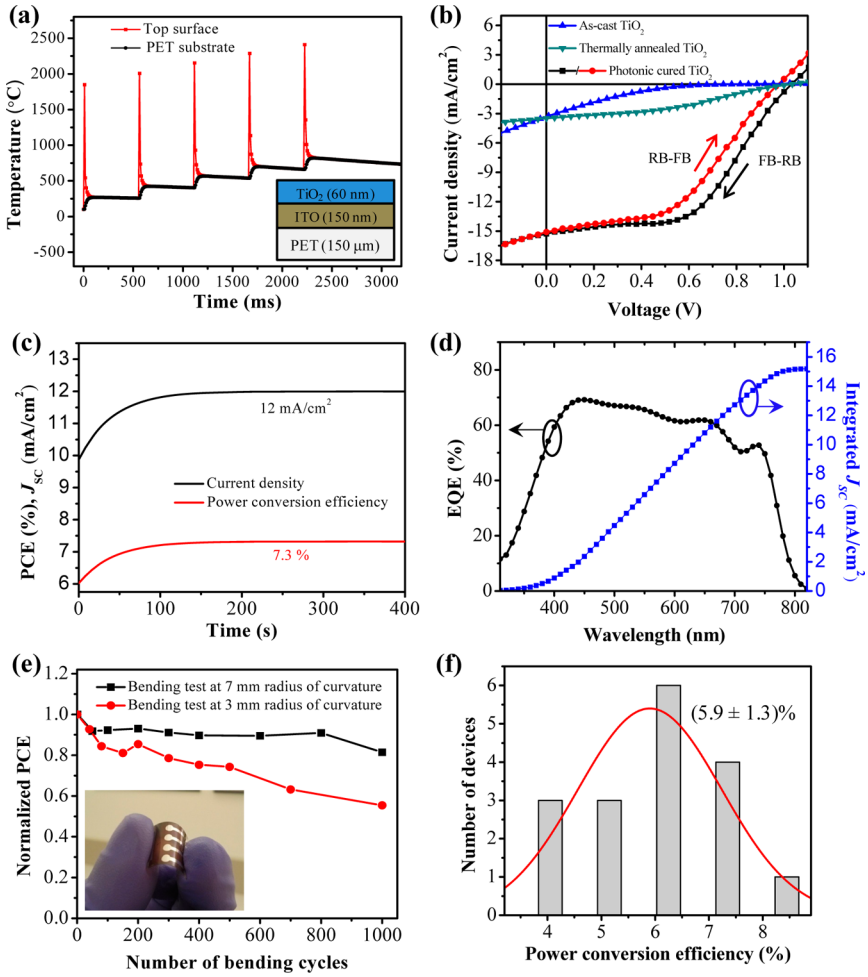

Figure 5. (a) Simulated temperature-versus-time profile for the photonic curing procedure used to anneal TiO_2 thin films on top of ITO/PET substrates. (b) Comparison of flexible device performances with as-deposited, thermally annealed, and photonic-cured TiO_2 films. (c) Current density and PCE as a function of time for the same device held at 0.61 V forward bias. (d) EQE spectrum and integrated J_{SC} for the flexible device with photonic-cured TiO_2 under short-circuit conditions. (e) Normalized PCE of flexible devices after bending tests performed at 7 mm and 3 mm radii of curvature. Inset of (e) shows a photographic image of the flexible devices. (f) Histogram of PCEs based on 18 flexible devices.

Device Fabrication. ITO-coated glass (15 Ω/□) and PET (60 Ω/□) substrates were cleaned sequentially by sonication in detergent, deionized water, acetone, and 2-propanol, followed by baking at 70 °C for 2 h. The as-prepared TiO_2 solution was spin-coated onto UV-ozone-treated ITO-coated glass and PET substrates at 2000 rpm for 40 s in air. Subsequently, glass substrates were annealed at 500 °C in a muffle furnace for 30 min. For the PET substrates, the TiO_2 films were annealed by exposing them to five infrared pulses under a radiant exposure of 17.3 J/cm^2 from a plasma arc lamp for 2 ms pulse dwell time using a PulseForge 3300 processing system from NovaCentrix. The $CH_3NH_3PbI_{3-x}Cl_x$ solution was ultrasonically spray-coated onto TiO_2/ITO-coated glass and PET substrates in ambient air using an ExactaCoat system (Sono-Tek Corporation) equipped with a 120 kHz nozzle. Substrates were kept at 75 °C during coating under optimized USC process, i.e., a path speed of 100 mm/s, a nozzle height of 5 cm, an atomizing gas pressure of 2.6 psi, and an infusion rate of 3.2 mL/min. After drying the coated films, they were annealed at 100 °C for an hour in air. For spin-coated devices, a 40 wt % $CH_3NH_3PbI_{3-x}Cl_x$ solution was spin-coated onto TiO_2/ITO-coated glass and PET substrates at 3000 rpm for 45 s and subsequently annealed at 100 °C for 1 h. The as-prepared Spiro-OMeTAD solution was spin-coated at 2000 rpm for 30 s on top of $CH_3NH_3PbI_{3-x}Cl_x$ films. Finally, a 100 nm thick Ag layer was thermally deposited at 1 Å/s under a vacuum level of 4×10^{-6} mbar, using a shadow mask to complete the devices. The device area of 6.5 mm^2 was calculated by a high-resolution optical microscope.

Film and Device Characterization. Current−voltage (J−V) curves of the fabricated solar cells were measured by scanning from forward bias to reverse bias (1.2 V to −0.2 V) direction and vice versa after a ∼120 s initial light soaking time, using a source meter (Keithley 2400, USA) and a solar simulator (Radiant Source Technology, 300 W, Class A) under the AM 1.5G (100 mW/cm^2) conditions. The intensity of the solar simulator was calibrated by a NIST-certified Newport Si reference cell. The voltage step during the scan was fixed at 35 mV with a delay time of 50 ms. EQE measurements were conducted in air using a Newport QE measurement kit under short-circuit conditions. X-ray diffraction measurement was done using a high-resolution PANalytical X'Pert Pro MPD diffractometer with a Cu Kα source (wavelength 1.540 50 Å). The film morphology was studied by a Zeiss Merlin VP scanning electron microscope.

DOI: 10.1021/acsphotonics.5b00119
ACS Photonics 2015, 2, 680−686

■ ASSOCIATED CONTENT

Supporting Information

Additional film characterization, device performance, and bending test data. The Supporting Information is available free of charge on the ACS Publications website at DOI: 10.1021/acsphotonics.5b00119.

■ AUTHOR INFORMATION

Corresponding Author

*E-mail: xiaok@ornl.gov.

Notes

The authors declare no competing financial interest.

■ ACKNOWLEDGMENTS

This research was conducted at the Center for Nanophase Materials Sciences (CNMS), which is a DOE Office of Science User Facility. S. D., P. J., and T. A. acknowledge support provided by a Laboratory Directed Research and Development award from Oak Ridge National Laboratory.

■ REFERENCES

(1) Kojima, A.; Teshima, K.; Shirai, Y.; Miyasaka, T. Organometal Halide Perovskites as Visible-Light Sensitizers for Photovoltaic Cells. *J. Am. Chem. Soc.* **2009**, *131*, 6050−6051.

(2) Jeon, N. J.; Noh, J. H.; Yang, W. S.; Kim, Y. C.; Ryu, S.; Seo, J.; Seok, S. I. Compositional Engineering of Perovskite Materials for High-Performance Solar Cells. *Nature* **2015**, *517*, 476−480.

(3) Zhou, H.; Chen, Q.; Li, G.; Luo, S.; Song, T.-b.; Duan, H.-S.; Hong, Z.; You, J.; Liu, Y.; Yang, Y. Interface Engineering of Highly Efficient Perovskite Solar Cells. *Science* **2014**, *345*, 542−546.

(4) Stranks, S. D.; Eperon, G. E.; Grancini, G.; Menelaou, C.; Alcocer, M. J.; Leijtens, T.; Herz, L. M.; Petrozza, A.; Snaith, H. J. Electron-Hole Diffusion Lengths Exceeding 1 Micrometer in an Organometal Trihalide Perovskite Absorber. *Science* **2013**, *342*, 341−344.

(5) Lee, M. M.; Teuscher, J.; Miyasaka, T.; Murakami, T. N.; Snaith, H. J. Efficient Hybrid Solar Cells Based on Meso-Superstructured Organometal Halide Perovskites. *Science* **2012**, *338*, 643−647.

(6) Liu, M.; Johnston, M. B.; Snaith, H. J. Efficient Planar Heterojunction Perovskite Solar Cells by Vapour Deposition. *Nature* **2013**, *501*, 395−398.

(7) Chen, C. W.; Kang, H. W.; Hsiao, S. Y.; Yang, P. F.; Chiang, K. M.; Lin, H. W. Efficient and Uniform Planar-Type Perovskite Solar Cells by Simple Sequential Vacuum Deposition. *Adv. Mater.* **2014**, *26*, 6647−6652.

(8) Malinkiewicz, O.; Yella, A.; Lee, Y. H.; Espallargas, G. M.; Graetzel, M.; Nazeeruddin, M. K.; Bolink, H. J. Perovskite Solar Cells Employing Organic Charge-Transport Layers. *Nat. Photonics* **2014**, *8*, 128−132.

(9) Eperon, G. E.; Burlakov, V. M.; Docampo, P.; Goriely, A.; Snaith, H. J. Morphological Control for High Performance, Solution-Processed Planar Heterojunction Perovskite Solar Cells. *Adv. Funct. Mater.* **2014**, *24*, 151−157.

(10) Docampo, P.; Ball, J. M.; Darwich, M.; Eperon, G. E.; Snaith, H. J. Efficient Organometal Trihalide Perovskite Planar-Heterojunction Solar Cells on Flexible Polymer Substrates. *Nat. Commun.* **2013**, *4*, 2761.

(11) Burschka, J.; Pellet, N.; Moon, S.-J.; Humphry-Baker, R.; Gao, P.; Nazeeruddin, M. K.; Grätzel, M. Sequential Deposition as a Route to High-Performance Perovskite-Sensitized Solar Cells. *Nature* **2013**, *499*, 316−319.

(12) Xiao, Z.; Bi, C.; Shao, Y.; Dong, Q.; Wang, Q.; Yuan, Y.; Wang, C.; Gao, Y.; Huang, J. Efficient, High Yield Perovskite Photovoltaic Devices Grown by Interdiffusion of Solution-Processed Precursor Stacking Layers. *Energy Environ. Sci.* **2014**, *7*, 2619−2623.

(13) Chen, Q.; Zhou, H.; Hong, Z.; Luo, S.; Duan, H.-S.; Wang, H.-H.; Liu, Y.; Li, G.; Yang, Y. Planar Heterojunction Perovskite Solar Cells via Vapor-Assisted Solution Process. *J. Am. Chem. Soc.* **2013**, *136*, 622−625.

(14) Sirringhaus, H.; Kawase, T.; Friend, R.; Shimoda, T.; Inbasekaran, M.; Wu, W.; Woo, E. High-Resolution Inkjet Printing of All-Polymer Transistor Circuits. *Science* **2000**, *290*, 2123−2126.

(15) Steirer, K. X.; Reese, M. O.; Rupert, B. L.; Kopidakis, N.; Olson, D. C.; Collins, R. T.; Ginley, D. S. Ultrasonic Spray Deposition for Production of Organic Solar Cells. *Sol. Energy Mater. Sol. Cells* **2009**, *93*, 447−453.

(16) Krebs, F. C.; Gevorgyan, S. A.; Alstrup, J. A Roll-To-Roll Process to Flexible Polymer Solar Cells: Model Studies, Manufacture and Operational Stability Studies. *J. Mater. Chem.* **2009**, *19*, 5442−5451.

(17) Wei, Z.; Chen, H.; Yan, K.; Yang, S. Inkjet Printing and Instant Chemical Transformation of a $CH_3NH_3PbI_3$/Nanocarbon Electrode and Interface for Planar Perovskite Solar Cells. *Angew. Chem., Int. Ed.* **2014**, *53*, 13239−13243.

(18) Kim, J. H.; Williams, S. T.; Cho, N.; Chueh, C. C.; Jen, A. K. Y. Enhanced Environmental Stability of Planar Heterojunction Perovskite Solar Cells Based on Blade-Coating. *Adv. Energy Mater.* **2014**, *5*, 1401229.

(19) Vak, D.; Hwang, K.; Faulks, A.; Jung, Y. S.; Clark, N.; Kim, D. Y.; Wilson, G. J.; Watkins, S. E. 3D Printer Based Slot-Die Coater as a Lab-to-Fab Translation Tool for Solution-Processed Solar Cells. *Adv. Energy Mater.* **2014**, *5*, 1401539.

(20) Hoth, C. N.; Choulis, S. A.; Schilinsky, P.; Brabec, C. J. High Photovoltaic Performance of Inkjet Printed Polymer:Fullerene Blends. *Adv. Mater.* **2007**, *19*, 3973−3978.

(21) Hoth, C. N.; Schilinsky, P.; Choulis, S. A.; Brabec, C. J. Printing Highly Efficient Organic Solar Cells. *Nano Lett.* **2008**, *8*, 2806−2813.

(22) Ju, J.; Yamagata, Y.; Higuchi, T. Thin-Film Fabrication Method for Organic Light-Emitting Diodes Using Electrospray Deposition. *Adv. Mater.* **2009**, *21*, 4343−4347.

(23) Tenent, R. C.; Barnes, T. M.; Bergeson, J. D.; Ferguson, A. J.; To, B.; Gedvilas, L. M.; Heben, M. J.; Blackburn, J. L. Ultrasmooth, Large-Area, High-Uniformity, Conductive Transparent Single-Walled-Carbon-Nanotube Films for Photovoltaics Produced by Ultrasonic Spraying. *Adv. Mater.* **2009**, *21*, 3210−3216.

(24) Girotto, C.; Moia, D.; Rand, B. P.; Heremans, P. High-Performance Organic Solar Cells with Spray-Coated Hole-Transport and Active Layers. *Adv. Funct. Mater.* **2011**, *21*, 64−72.

(25) Tedde, S. F.; Kern, J.; Sterzl, T.; Furst, J.; Lugli, P.; Hayden, O. Fully Spray Coated Organic Photodiodes. *Nano Lett.* **2009**, *9*, 980−983.

(26) Shao, M.; Das, S.; Xiao, K.; Chen, J.; Keum, J. K.; Ivanov, I. N.; Gu, G.; Durant, W.; Li, D.; Geohegan, D. B. High-Performance Organic Field-Effect Transistors with Dielectric and Active Layers Printed Sequentially by Ultrasonic Spraying. *J. Mater. Chem. C* **2013**, *1*, 4384−4390.

(27) Lefort, M.; Popa, G.; Seyrek, E.; Szamocki, R.; Felix, O.; Hemmerlé, J.; Vidal, L.; Voegel, J. C.; Boulmedais, F.; Decher, G. Spray-On Organic/Inorganic Films: A General Method for the Formation of Functional Nano- to Microscale Coatings. *Angew. Chem., Int. Ed.* **2010**, *49*, 10110−10113.

(28) Ishikawa, T.; Nakamura, M.; Fujita, K.; Tsutsui, T. Preparation of Organic Bulk Heterojunction Photovoltaic Cells by Evaporative Spray Deposition from Ultradilute Solution. *Appl. Phys. Lett.* **2004**, *84*, 2424−2426.

(29) Barrows, A. T.; Pearson, A. J.; Kwak, C. K.; Dunbar, A. D.; Buckley, A. R.; Lidzey, D. G. Efficient Planar Heterojunction Mixed-Halide Perovskite Solar Cells Deposited via Spray-Deposition. *Energy Environ. Sci.* **2014**, *7*, 2944−2950.

(30) Xiao, Z.; Dong, Q.; Bi, C.; Shao, Y.; Yuan, Y.; Huang, J. Solvent Annealing of Perovskite Induced Crystal Growth for Photovoltaic Device Efficiency Enhancement. *Adv. Mater.* **2014**, *26*, 6503−6509.

DOI: 10.1021/acsphotonics.5b00119
ACS Photonics 2015, 2, 680−686

(31) Chen, Y.; Chen, T.; Dai, L. Layer-by-Layer Growth of $CH_3NH_3PbI_{3-x}Cl_x$ for Highly Efficient Planar Heterojunction Perovskite Solar Cells. *Adv. Mater.* **2015**, *27*, 1053−1059.
(32) Xiao, M.; Huang, F.; Huang, W.; Dkhissi, Y.; Zhu, Y.; Etheridge, J.; Weale, A. G.; Bach, U.; Cheng, Y. B.; Spiccia, L. A Fast Deposition-Crystallization Procedure for Highly Efficient Lead Iodide Perovskite Thin-Film Solar Cells. *Angew. Chem., Int. Ed.* **2014**, *126*, 10056−10061.
(33) Snaith, H. J.; Abate, A.; Ball, J. M.; Eperon, G. E.; Leijtens, T.; Noel, N. K.; Stranks, S. D.; Wang, J. T.-W.; Wojciechowski, K.; Zhang, W. Anomalous Hysteresis in Perovskite Solar Cells. *J. Phys. Chem. Lett.* **2014**, *5*, 1511−1515.
(34) Wojciechowski, K.; Stranks, S. D.; Abate, A.; Sadoughi, G.; Sadhanala, A.; Kopidakis, N.; Rumbles, G.; Li, C.-Z.; Friend, R. H.; Jen, A. K.-Y. Heterojunction Modification for Highly Efficient Organic−Inorganic Perovskite Solar Cells. *ACS Nano* **2014**, *8*, 12701−12709.
(35) Nguyen, W. H.; Bailie, C. D.; Unger, E. L.; McGehee, M. D. Enhancing the Hole-Conductivity of Spiro-OMeTAD without Oxygen or Lithium Salts by Using $Spiro(TFSI)_2$ in Perovskite and Dye-Sensitized Solar Cells. *J. Am. Chem. Soc.* **2014**, *136*, 10996−11001.
(36) Rivard, J.; Sabau, A.; Blue, C. A.; Ohriner, E. K.; Jayaraman, N. Thermophysical Properties of Roll-Compacted Nickel Sheet for High-Density Infrared Sheet Fabrication. *Metall. Mater. Trans. A* **2003**, *34*, 3043−3054.
(37) Sabau, A. S.; Kadolkar, P. B.; Dinwiddie, R. B.; Ott, R. D.; Blue, C. A. Process Parameters for Infrared Processing of FePt Nanoparticle Films. *Metall. Mater. Trans. A* **2007**, *38*, 788−797.

DOI: 10.1021/acsphotonics.5b00119
ACS Photonics 2015, 2, 680−686